BMC Cancer

RESEARCH Open Access

BRAF mutations and the association of V600E with CD133 and CDX2 expression in a Pakistani colorectal carcinoma cohort

Sobia Hassan[1], Talat Mirza[2], Ambrina Khatoon[3*], Uzma Bukhari[4], Fouzia Shaikh[1] and Asad Karim[5]

Abstract

Background Despite a high incidence of colorectal carcinoma, data regarding genetic aberrations in colorectal carcinoma (CRC) patients in Pakistan is scarce. This study aimed to determine the frequency of *BRAFV600E* mutations in colorectal carcinoma tissue in the Pakistani population and to associate *BRAFV600E expression* with *CD133*, a marker of colorectal stem cells, and *CDX2* marker of differentiation.

Methods Sanger Sequencing of exon 15 (426 bp) including the hotspot *V600E* was performed on formalin-fixed-paraffin-embedded (FFPE) CRC tissue samples of 115 patients. The samples were subjected to immunohistochemistry (IHC) to assess the expression of *BRAFV600E*, *CDX2*, and *CD133*. Additionally, homology modelling and docking were performed to investigate novel deletions revealed in sequencing.

Results Twenty-four (20.8%) *BRAF* variants were identified in the coding region, with *V600E* mutations detected in 14 (12.2%)cases (GenBank: PP003258.1; Pop Set: 2678087296). Moreover, a wide spectrum of novel non-*V600E* mutations (8.6%) were identified, including deletions and missense variations. In-silico analysis revealed that due to large deletions in the coding region of three samples, the affinity of the anti-*BRAF* drugs (Encorafenib and Vemurafenib) for the active site decreased in comparison to the wild type. The IHC analysis showed that *BRAFV600E* expression was significantly associated with *CD133* expression ($\chi^2_{(1, n=115)} = 26.351$; p = < 0.001) and with *CDX2* expression ($\chi^2_{(1, n=115)} = 14.88$; $p = 0.001$). Multivariate analysis using binary logistic regression revealed association of *BRAFV600E* mutations with age (OR = 1.123; CI = 1.024–1.232; $p = 0.014$), gender (OR = 0.071; CI = 0.006–0.831; $p = 0.035$), grade (0.007; CI = 0-0.644) and *CD133* expression (OR = 65.649; CI = 2.153-2001.556; $p = 0.016$).

Conclusion The present study demonstrates a notably high *V600E* frequency (12.2%) in comparison to global reported data, which ranges from 0.4 to 18%. This finding reflects the importance of upfront *BRAF* testing of the genetically distinct population of Pakistan. Previously unreported mutations identified in the sample may be of clinical significance and warrant further investigation. The concomitant high expression and significant association between *CD133* and *BRAFV600E* represent vital actionable genes that may be targeted together to improve CRC patient management.

Keywords Colon cancer, Genetic, Polymorphism, *Prominin*-1, Cancer stem cells, Vemurafenib, Encorafenib

*Correspondence:
Ambrina Khatoon
ambrina.khatoon@zu.edu.pk

Full list of author information is available at the end of the article

Introduction

Colorectal cancer (CRC) ranks as the third most commonly diagnosed cancer globally, with both its incidence and mortality projected to increase in the coming decades. While high-income countries currently bear a substantial burden of CRC-related deaths, developing countries are also witnessing a rise in CRC cases and fatalities [1]. Early detection of CRC allows for a complete cure through surgery and subsequent medications [2]. However, it is important to note that the recurrence rate is high, and the development of drug resistance poses a significant risk of treatment failure [1, 2]. CRC exhibits considerable genetic diversity, with various mutations influencing prognosis and responses to different targeted treatments. Notably, mutations in the RAS and *BRAF* genes are crucial for clinical decision-making [3]. *BRAF* gene, a protooncogene, regardless of *RAS* mutation, plays a key role in tumour cell proliferation via the MAP-kinase pathway [3]. The association of *BRAF* gene mutation with CRC has been documented to be an independent molecular event and represents a notable actionable genetic alteration [4]. *BRAF* mutations in metastatic CRC (mCRC) patients have been documented to be a negative predictor of anti-*EGFR* therapy [5]. The National Comprehensive Cancer Network guidelines recommend testing for *BRAF* mutation in mCRC patients. Molecular profiling and the use of targeted drugs have widely improved cancer survival [6]. Clinical trials have been conducted using anti-EGFR drugs like vemurafenib and encorafenib in an attempt to overcome *BRAF*-associated resistance to therapy [6]. The BEACON trial revealed promising outcomes on co-targeting *BRAF* and EGFR with encorafenib and cetuximab in mCRC cases bearing *BRAFV600E* mutations. Combined therapy with these two drugs has been established as the new standard of care regimen for patients with *BRAF V600E* mCRC [7].

CDX2, a homeobox transcription factor, has been reported to be a differentiation marker. In healthy individuals, *CDX2* expression has been observed in the nuclei of colonic epithelial cells and is considered to be essential for intestinal growth and differentiation [8] while the loss of expression in CRC has been associated with a more advanced stage of the tumour [9]. Choi et al. reported CRCs with the *BRAFV600E* mutation exhibited lower *CDX2* expression compared to CRCs without this mutation. Additionally, their study revealed that patients with *CDX2* expression had improved overall and cancer-specific survival rates compared to those lacking *CDX2* expression [10]. As differentiation-promoting *CDX2* levels decrease, there is a retention of stem cells [11]. Cancer stem cells (CSCs) have been established to have tumourigenic potential and are considered to contribute to therapy resistance and progression of CRC after the surgical resection of primary growth [12]. The resilience of colorectal CSCs to conventional treatments contributes to the aggressiveness of CRC [13]. Therefore, the identification of CSCs may be helpful in the search for therapeutic targets and useful prognostic markers for CRC. Among the reported makers of cancer stem cells, *CD133* is a well-known marker for isolating and studying cancer stem cells in various cancers [14]. *CD133* is a glycosylated transmembrane protein, encoded by *PROM1* "Prominin-1" and has been proposed to be a therapeutic target [15]. Silencing of *CD133* has been reported to reduce tumour cell migration and stemness properties in CRC cell lines [16]. Furthermore, targeting *CD133* has been associated with overcoming drug resistance [13]. A study on anaplastic thyroid cancer cell lines documented *BRAFV600E* mutation to be associated with *CD133*-positive CSCs [17]. The identification of *CD133* overexpression in *BRAF* mutant CRC patients may identify a sub-group of tumours that may respond to a combination of *BRAF* inhibitors and anti-*CD133* drugs.

Since the clinical decision-making and treatment response is based upon the underlying genetic aberrations, it has been recommended to do genetic testing before starting systemic therapy in metastatic CRC [18]. To the best of our knowledge, there are no reported studies on *BRAF* mutations in CRC patients in Pakistan. This study focuses on key molecular events, *BRAF* mutations, *CDX2* loss, and *CD133* expression which may be adding to the mortality rate of CRC due to their association with poor prognosis, tumour proliferation, and therapy resistance. This study aimed to determine the frequency of *BRAFV600E* mutations in the Pakistani population and to find out the association between *BRAFV600E* and colorectal cancer stemness using *CD133* as a marker of CRC stem cells and *CDX2* a marker of differentiation. Moreover, it aimed to determine the association of *BRAFV600E*, *CD133* expression, and *CDX2* expression with various clinicopathologic features.

Methodology

Ethics approval

The study was conducted in accordance with the Helsinki Declaration and was authorized by the Ethics Review Board, Ziauddin University, Karachi, Pakistan (2861120SHPAT29.01.2021).

Informed consent

After, ethical approval, written informed consent was taken from study participants and the data collected was kept confidential.

Study participants & setting

This analytic cross-sectional study was conducted at the multidisciplinary laboratory, Ziauddin University, Karachi, Pakistan, and Dow Diagnostic Reference

and Research Laboratory, Dow Institute of Health Sciences, Karachi, Pakistan from January 2021 to December 2023. After informed consent, 115 colorectal carcinoma patients, comprising adults (above 18 years) of both genders, were enrolled in the study. Only the cases of primary CRC with no history of chemo or radiotherapy were included in the study, regardless of the metastatic status of the case. Moreover, the samples which showed poor fixation of tissue were excluded. All histological slides were screened by experienced pathologists to retrieve sections that were best representative of colorectal adenocarcinoma in each patient. Clinicopathologic data was recorded which included age, gender, tumour laterality, grade, pathologic stage, and perineural and lymphovascular invasion.

DNA extraction

Manual DNA extraction was done from FFPE tissue samples. The FFPE tissue sections representative of the tumour area, were transferred to the microcentrifuge tube and deparaffinized using 800 µl xylene. The tube was incubated at room temperature for 30 min while tapping in between. This was followed by centrifugation at 14,000 rpm for 3 min and the xylene was then discarded. The xylene was added again and the same steps were repeated. After removing xylene from the tubes, ethanol rehydration was performed using 800 µl absolute ethanol. The sample was vortexed and then put into centrifugation for 3 min. These steps were repeated using 70% ethanol and then with 50% ethanol, followed by centrifugation at 14,000 rpm for 5 min. The ethanol was discarded and the sample was left to air dry for about 20 min (or till the sample was dry). For tissue digestion lysis buffer [1.4 M NaCl, 100mM Tris-HCl pH 8.0,20 mM EDTA pH 8.0, CTAB (Cetyl trimethyl ammonium bromide), B-mercaptoethanol and proteinase K] was used. An addition of 1 ml of warm CTAB buffer was made to the microcentrifuge tube. Then 20 µl protein kinase was added and the tube was incubated at 60 °C for up to 3 h (till the sample was digested), adding 10 µl protein kinase every hour. The sample was allowed to rest at room temperature for 10 min. For DNA clean-up, chloroform: isoamyl alcohol (24:1) was added, mixing gently by inverting the tube several times and put to centrifugation at 14,000 rpm for 5 min. The supernatant was carefully removed and transferred to another tube. About 2/3 volume of chilled isopropanol was added and mixed gently. The tube was inverted up and down to visualize the DNA thread. The tube was kept at -20^{0}C for 30 min. Centrifugation at 14,000 rpm for 10 min was done. The supernatant was discarded. The pellet was washed with 100 µl chilled 70% ethanol and centrifuged at 10,000 rpm for 20 min. After decanting the supernatant and the pellet was air-dried at room temperature. The addition of 100 µl of Tris EDTA was done and the sample was tapped to resuspend the pellet. For quantification, a Multiskan Sky spectrophotometer was used and purity was calculated as the ratio of A260/280. The integrity of extracted DNA was checked using gel electrophoresis.

Polymerase chain reaction (PCR)

DNA amplification was done using PCR. Primers flanking a 426-bp amplicon of *BRAF* exon 15 encompassing the V600 codon were designed. Forward primer, 5'AACTCAGCAGCATCTCAGGG3' and reverse primer 5'AGCATCTCACCTCATCCTAACA3' were used. The designed primer also covered the flanking intronic regions of the *BRAF* exon 15. For PCR cycles, initial denaturation was done at 95^{0}C for 5 min followed by 35 cycles of 1 min at 95^{0}C, 1 min at 59.5^{0}C, and 1 min at 72^{0}C with a final extension of 5 min at 72^{0}C. Submerged 2% agarose gel electrophoresis was used to observe the amplification products.

Sanger sequencing and bioinformatic analysis

Sanger sequencing was used to analyze *BRAF* exon 15 (Size 426 bp). The sequencing procedure was outsourced and performed with Lab Genetic, Lahore. MEGA X software was used for sequence alignment and trimming. All sequences were aligned using NCBI Blastn and Blastp.

Predicting protein structure and molecular docking

Based on the results, the study was further elaborated to identify the significance of novel findings. BRAF protein contains 281 amino acids out of which 39 are coded by exon 15. The protein Crystal structure of the BRAF (R509H) kinase domain monomer (PDP ID: 4RZV) bound to ligands (vemurafenib) was downloaded from the PDB database and used as a reference. This structure was used for induced fit docking using the same bounded vemurafenib, to explore the interaction between protein and ligand. To study the effect of binding of drugs to mutant proteins, the reference sequence was modified according to the mutations identified in samples ZU-COL-27, ZU-COL-35, and ZU-COL-37. Then 3D structure of these modified proteins was built via homology modeling using Swiss-model. The OPLS4 force field was applied to minimize the structures and the validation of the protein 3D structures was done using the Procheck server (https://saves.mbi.ucla.edu/to). The 3D structure of the reference (wild type) BRAF (R509H) kinase domain monomer protein was compared with the mutant proteins (ZU-COL-27, ZU-COL-35, and ZU-COL-37) using the quick alignment option in Maestro (Schrodinger) software. We used the SiteMap option in Maestro (Schrodinger) software to explore possible druggable pockets on the mutated protein surface under the OPLS4 force field with default settings. The druggable pockets

having residues involved in protein-ligand interaction in the reference protein were selected for docking of vemurafenib with modified reference protein; 3D structure of ZU-COL-27, ZU-COL-35, and ZU-COL-37, respectively. We also performed docking of drug encorafenib with wild type BRAF (R509H) kinase domain monomer and the three mutant proteins. LigPre application in maestro software was used to prepare tautomers for the encorafenib and vemurafenib.

Immunohistochemical analysis

Immunohistochemistry (IHC) was performed with standard procedures using antibodies against *CDX2*, *CD133*, *and BRAFV600E.* Poly-lysine-coated slides were used for mounting tissue sections of about 4 µm thickness from formalin-fixed paraffin-embedded blocks. After drying at 56^0C for 30 minutes, the tissue sections were deparaffinized using 100% xylene, three times for 5 minutes each, followed by rehydration in serial ethanol grades (100%, 90%, 70%, and 50%). Unmasking of antigen was performed by placing slides in a container filled with citrate buffer pH 6.0 positioned in a pressure cooker. After the whistle, the samples were kept in the cooker for 8 minutes followed by 30 minutes of cooling at room temperature. The endogenous peroxidase activity was blocked by immersing slides in 3% hydrogen peroxide containing sodium azide for five minutes. Following washing by PBS, tissue slides were incubated with anti-*CDX2* monoclonal mouse antibody (Dako, IR08061-2, clone DAK-*CDX2*) for 30 minutes while anti-*CD133* polyclonal antibody (Invitrogen MA-PA5-82184) and *BRAF* recombinant rabbit monoclonal antibody (Invitrogen MA5-24661) were incubated for 60 minutes at room temperature. Tissue sections were washed with PBS and incubated with HRP-labelled secondary antibody (Envision$^+$, Dako) for 30 min. After cleaning tissue sections with PBS, the antigen-antibody reaction substrate chromogen solution was applied. Sections were developed with DAB (3, 4, 3', 4' - tetra amino biphenyl hydrochloride) for five minutes at 37^0C, after washing, counter-staining was done using Mayer Hematoxylin for one minute. The sections were subjected to running water for ten minutes before decolorizing in 1% acid alcohol. Specimens were dried using graded alcohol concentrations (70%, 80%, 95%, and 100%) for two minutes, followed by cleaning in xylene: phenol (1:1) solution, with two changes of xylene for two minutes individually and lastly fixed in DPX. For quality management, positive and negative controls for all cases were run. The placenta was taken as a positive control of *CD133* while the normal colon was taken as a control for *CDX2*. The positive control used for *BRAF* was papillary thyroid carcinoma with documented *BRAF V600E* mutation, as per the manufacturer's protocol. Immunoreactivity was scored by considering the percentage of stained tumour cells (yellowish-brown colour). Scoring was done at 400 magnification by three independent pathologists with blinding of clinicopathologic characteristics. In cases with discrepancies, cases were re-evaluated and discussed until a consensus was reached. For *BRAF*, immunoreactivity was taken as positive when more than 10% of tumour cells showed uniform cytoplasmic staining [19]. For *CDX2*, less than 25% staining was considered a loss of *CDX2* [20]. For the scoring of *CD133*, the product of the score of staining intensity and the percentage of positive cells were taken. The percentage of positive cells was scored as 0=no positive cells; 1=1–20% positive cells; 2=21–50% positive cells; 3=51–70% positive cells; and 4=71% and more positive cells. The staining intensity was graded as 0=no staining of cancer cells; 1=weak staining; 2=moderate staining; and 3 strong staining. The immunoreactivity score of less than four was considered as low expression while a score of four and above was taken as high *CD133* expression [21].

Statistical analysis

Statistical analysis was done using SPSS version 24.0 (IBM Corp., New York, NY, USA). Statistics were used to include the frequencies and percentages of categorical variables and mean and standard deviation for quantitative data.*CD133* expression was compared with different clinicopathologic features using the chi-square/Fischer exact test. Pearson's Chi-square test was used to determine the association of *BRAFV600E* expression with *CD133* and *CDX2* expression. A Heatmap of the obtained immunoscore was constructed using GraphPad Prism. Binary logistic regression analysis was performed to assess the relationship of clinicopathologic variables with *BRAFV600E*. For univariate analysis, a p-value of ≤0.25 was considered statistically significant. The significant results from univariate analysis were included in the multivariate analysis model and a p-value of ≤0.05 was taken as significant.

Results

Patient demographics

Clinicopathologic features of CRC adenocarcinoma are given in Table 1. The age range of the sample was 75 years with minimum age recorded as 18 years and maximum 93 years, with a mean 47.82 ± 15.37 years. It was observed that most of the cases were younger than 50 years of age (52.2%). Out of the total 115 patients, 53 (46.1%) were females and 62 (53.9%) males. More than one-half of the cases were from the right colon region (53%). Most of the cases were found to be low-grade adenocarcinoma (87.8%) with pathologic tumour stages of T1–T3 (87%).

Lymphovascular invasion was observed in 56 (48.7%) cases while perineural invasion was present in 13(11.3%) cases. *BRAFV600E* mutation was found in 14(12.2%)

Table 1 Clinicopathologic features of colorectal adenocarcinoma patients ($n=115$)

Variables			Mean ± SD / Frequency (%)
Age			47.82 ± 15.37
Age groups	*< 50 years*		60(52.2%)
	≥ 50 years		55(47.8%)
Laterality	*Right colon*		61 (53%)
	Left colon		54(47%)
Gender	*Female*		53 (46.1%)
	Male		62 (53.9%)
Grade	*Low (well /moderately differentiated)*		101(87.8%)
	High (poorly differentiated)		14(12.2%)
pT stage	*T1-T3*		100 (87%)
	T4		15 (13%)
LVI	*Absent*		59(51.3%)
	Present		56(48.7%)
PNI	*Absent*		102(88.7%)
	Present		13(11.3%)
BRAF Mutational status	*Wild-Type*		91(79.1%)
	Substitution mutations	Non-*V600E*	4(3.5%)
		V600E	14(12.2%)
	Deletions		6(5.2%)
BRAFV600E Expression	*less than 10% (Negative)*		101(87.8%)
	10% and above (Positive)		14(12.2%)
CD133 Expression	*Low expression (PI < 4)*		92(80%)
	High expression (PI ≥ 4)		23(20%)
CDX2	*No loss (25% and above)*		93(80.9%)
	Loss of CDX2 (< 25%)		22(19.1%)

pT stage = pathologic tumour stage; PNI = Perineural invasion; LVI = lymphovascular invasion; BRAF = B-Raf (rapidly accelerated fibrosarcoma) proto-oncogene, CD133 = cluster of differentiation 133; CDX2 = caudal-type homeobox transcription factor 2

cases which was also detected in immunohistochemistry (Fig. 1). IHC activity showed high *CD133* expression in 23(20%) cases and loss of *CDX2* in 22 cases (19.1%).

BRAF sequencing

In the selected region of *BRAF* exon 15, a total of 24 exonic and 5 intronic variants were identified. Among the exonic mutations, 14 were *V600E* variants, and 10 were non-*V600E* variants. The *V600E* mutations exhibited a T>A substitution at nucleotide 1799 (GenBank: PP003258.1; Pop Set: 2678087296), resulting in the substitution of valine (V) with glutamic acid (E) at codon 600. The non-*V600E* mutations included both substitutions and deletions. The identified SNPs were classified as missense mutations and further analyzed using ClinVar, where these mutations were predominantly reported as pathogenic or likely pathogenic (Table 2). An exception was SNP rs12121336, identified in three cases, showing a novel mutation involving the deletion of allele A at position 14,753,345 (L597del). Despite this novel deletion, it has been reported in ClinVar as pathogenic or likely pathogenic based on missense variation. Moreover, the rs2128998256 missense variant was also observed but not documented in ClinVar. Additionally, two SNPs, rs121913363 and rs121913373, coexisted in a single case (ZU-COL-47) and have been documented as likely pathogenic in melanoma.

Moreover, previously unreported deletion mutations were detected in four samples. One sample exhibited a 1 bp deletion at position 140,753,287, leading to a frameshift mutation affecting codons 617–620. In sample ZU-COL-27, the deletion spanned 267 bp (140753296–140753563), while in ZU-COL-35, the deletion covered 260 bp (140753295–140753555), and in ZU-COL-37, the deletion extended over 276 bp (140753297–140753573). The large deletions identified in these three samples were further analysed through protein structure prediction.

Protein homology modeling

Homology modeling was used to build the 3D structure for ZU-COL-27, ZU-COL-35, and ZU-COL-37 protein sequences. All the predicted 3D structures were verified using Procheck server (https://saves.mbi.ucla.edu/to); VERIFY3D (At least 80% of the amino acids have scored >= 0.1 in the 3D/1D profile) and ERRAT2 (overall quality factor was ≥92. We used the BRAF (R509H) kinase domain monomer (PDB ID: 4RZV) 3D structure as a reference and aligned it with the 3D structures of the mutant BRAF proteins: ZU-COL-27(A), ZU-COL-35(B), and ZU-COL-37(C). The findings reveal that the

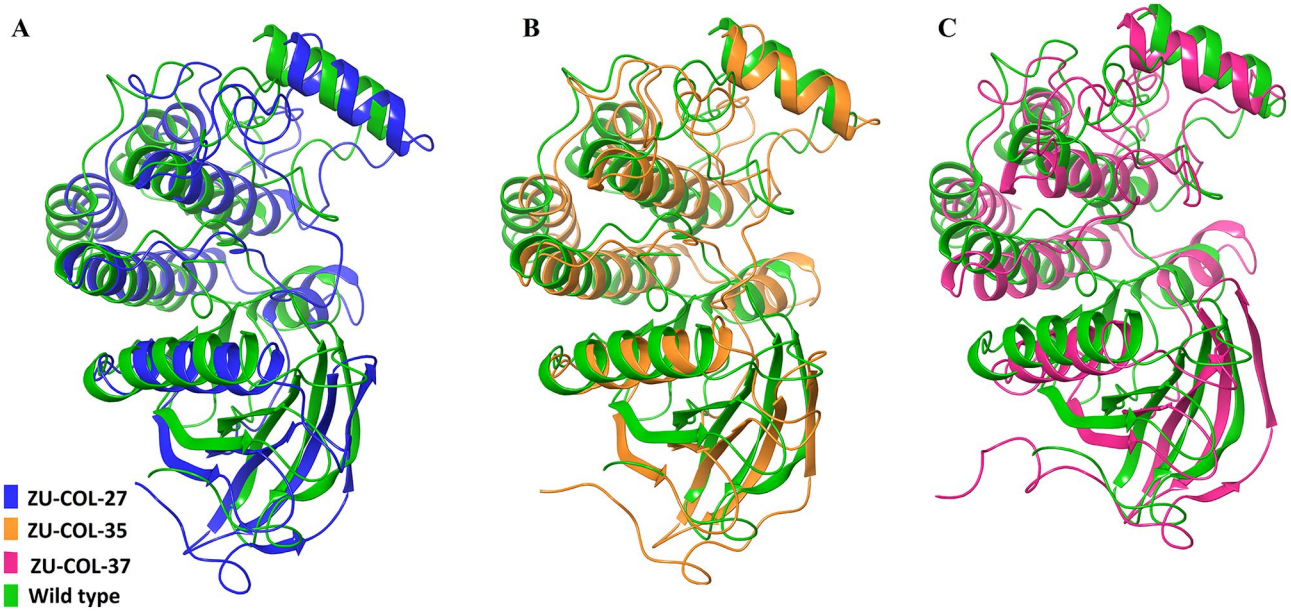

Fig. 1 The alignment of the wild-type BRAF protein with three mutant 3D structures, including ZU-COL-27 (**A**), ZU-COL-35 (**B**), and ZU-COL-37 (**C**)

Table 2 Single nucleotide polymorphisms identified in BRAF Gene and their clinical significance as reported in ClinVar

SNPs	Patient ID	ClinVar	Position	Protein change
rs121913366[+]	ZU-COL-28 ZU-COL-41 ZU-COL-43	LP/P[+]	140,753,345	p. Leu597del
rs121913363	ZU-COL-47	LP	140,753,361	p. Ile592Val
rs121913373	ZU-COL-47 ZU-COL-73	LP	140,753,321	p. Ser605Asn
rs121913335		LP	140,753,375	p. Asp587Ala
rs2128998256	ZU-COL-78	-Not reported-	140,753,330	p. Ser602Cys
rs113488022	ZU-COL-58, ZU-COL-59, ZU-COL-61, ZU-COL-63, ZU-COL-64, ZU-COL-67, ZU-COL-68, ZU-COL-70, ZU-COL-80, ZU-COL-81, ZU-COL-82, ZU-COL-83, ZU-COL-84, ZU-COL-85	P	140,753,336	p. Val600Glu

LP = Likely Pathogenic; P = Pathogenic

The table shows the SNPs identified in this study and their significance in pathogenicity reported by ClinVar. rs2128998256 is unreported on ClinVar

BRAFV600E is denoted by rs113488022 which was found in 14 patients

[+] = represents SNP which has been reported in ClinVar as a missense variant with the potential of being pathogenic or likely pathogenic. In our sample, this SNP showed deletion of leucine at codon 597 resulting in frameshift mutation which is a novel finding

mutations in the protein sequences resulted in alterations in the 3D structures of the proteins (Fig. 2).

Figure 3A shows the 3D structure of the protein and the interaction of the ligand with the protein (the green dotted line indicates a good interaction within the ligand-protein complex). Additionally, as indicated by the arrow, the ligand interacts more extensively with the protein through hydrophobic and polar interactions. The amino acids of the BRAF protein domain encoded by exon 15 are highlighted in pink and orange. The amino acid residues in orange are involved in protein-ligand binding. Similarly, the amino acid residues shown in red are also involved in protein-ligand interactions but are not encoded by exon 15. Figure 3B shows the 281-amino-acid sequence of the BRAF protein. Residues highlighted in orange and pink (39 amino acids) are encoded by exon 15, while residues highlighted in orange and red are involved in protein-ligand interactions.

It is important to note that when we performed protein-ligand docking for all three mutated proteins mentioned above with encorafenib and vemurafenib (Table 3), the highest docking score was observed for the wild type, while the binding affinity of the drugs decreased for the three mutant proteins. For instance, encorafenib's Tautomer 1 showed strong binding affinity for the wild type (-3.199 Kcal/mol) compared to the mutants: ZU-COL-27 (-3.146), ZU-COL-35 (-0.706), and ZU-COL-37 (-2.462). Similarly, vemurafenib binds more strongly to the wild type (-5.426 Kcal/mol) with a significant decrease in affinity for the mutant proteins, particularly ZU-COL-35 (-0.058 Kcal/mol). These findings suggest that the amino

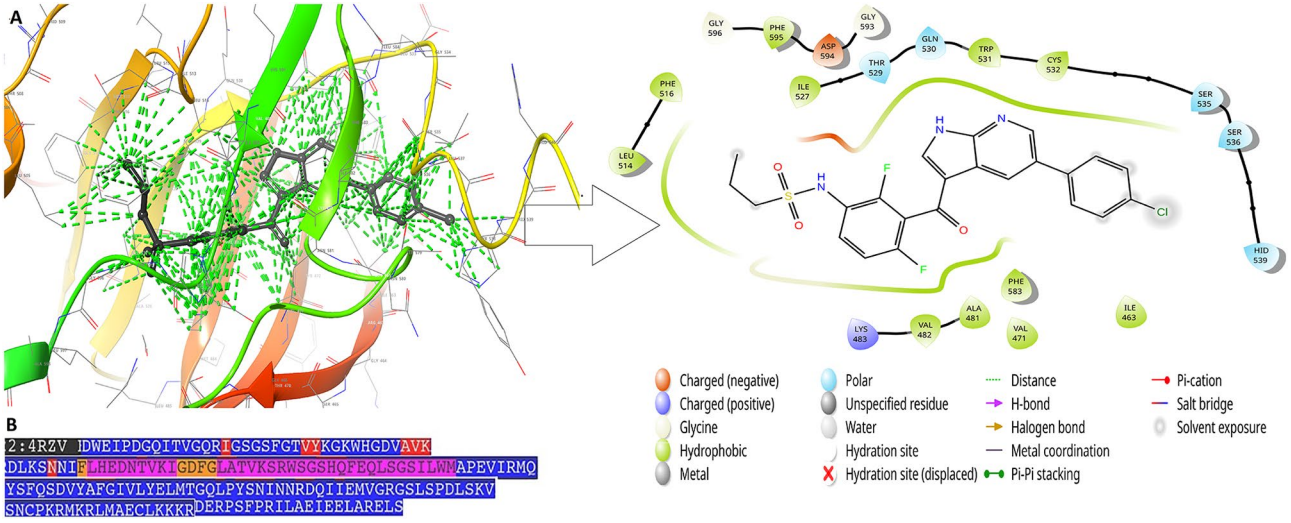

Fig. 2 The 3D and 2D structure (indicated with an arrow) of the BRAF-vemurafenib complex (**A**) is depicted, along with the 281 amino acid sequence of the BRAF protein (**B**)

acids encoded by exon 15 play an important role in drug binding.

Immunohistochemical analysis

The frequency of positive *BRAFV600E*, high *CD133*, and loss of *CDX* 2 expression is depicted in the Heatmap (Fig. 4) while Fig. 1 illustrates H&E and IHC. Based on IHC, the association of *CD133* and *CDX2* expression with independent variables was evaluated (Table 4). *CD133* expression revealed no association with age groups and gender ($p>0.05$) while there was a significant association of high *CD133* expression with the right-sided tumours ($p=0.002$), high grade ($p=0.001$), pT4 stage (0.002), positive lymphovascular ($p=0.01$) and perineural invasion ($p=0.022$). There was a significant association of high grade ($p=0.001$), pT4 stage ($p=0.009$) and positive perineural invasion ($p=0.017$). However, no association was observed between CDX2, age, gender, location or lymphovascular invasion ($p>0.05$). All cases with *BRAFV600E* mutations showed positive immunohistochemical reactivity with anti-*BRAFV600E* antibody. A highly significant association of *BRAFV600E* expression with *CD133* expression with ($\chi^2_{(1,\ n=115)}=26.31$; p=<0.001) and *CDX2* expression was observed ($\chi^2_{(1,\ n=115)}=14.88$; $p=0.001$) (Table 5).

Binary logistic regression analysis for BRAFV600E mutations

Univariate and multivariate analysis was done with a 95% confidence interval to determine if clinicopathologic variables can predict the likelihood of *BRAFV600E* mutations. On univariate regression analysis, it was observed that as the age increases by 1 year, the odds of *BRAFV600E* mutation will increase by 7.7% ($p=0.002$) (Table 6). The male gender was observed to be 88.6% less likely to have *BRAFV600E* mutation as compared to females($p=0.006$). The left-sided location of CRC was 84.3% less likely to show *BRAFV600E* as compared to right-sided CRC($p=0.019$). As compared to low-grade tumours, the high-grade tumours were found to be 47.9% times less likely to have *BRAFV600E* mutation ($p=0.545$). It was observed that the pT4 stage is 7.66 times more likely to exhibit *BRAFV600E* mutations as compared to pT1-pT3 ($p=0.002$). High *CD133* expression was found to be 16.9 times more likely to show *BRAFV600E* mutations as compared to low *CD133* expression. Loss of *CDX2* was observed to be 8.28 times more likely to show *BRAFV600E* mutation ($p=0.001$) as compared to cases with no loss of *CDX2*. However, on multivariate regression analysis, it was revealed that the likelihood of *BRAFV600E* mutation increases significantly with advancing age ($p=0.014$), female gender ($p=0.035$), lower tumour grade ($p=0.31$) and *CD133* ($p=0.016$). There was no significant association of the likelihood of *BRAFV600E* mutation with tumour laterality, pathologic tumour stage and loss of *CDX2* expression ($p>0.05$) (Table 6).

Discussion

BRAFV600E mutations in CRC have been documented to be an early event and targeting such mutations early in the course of the disease can support precision medicine [22, 23]. The reported frequency of *BRAF* mutations in CRC patients varies among different geographical regions with a higher number of *BRAF* mutations in countries like Denmark (18%), Turkey (12.9%), and India (17%) [24–26]. There has been a relatively lower frequency reported by China (4.15%) and Saudi Arabia (0.4%) [4, 27]. Similar

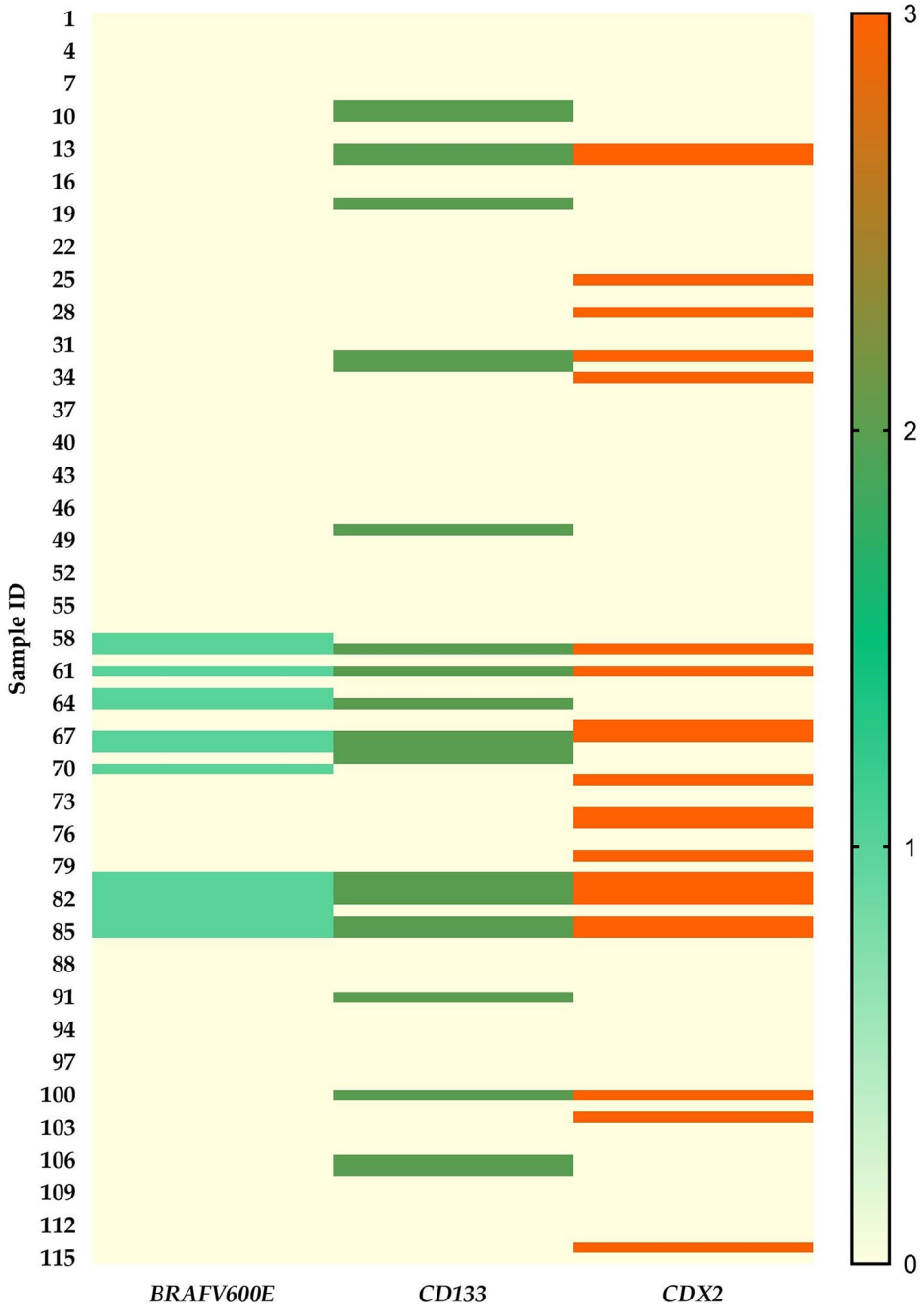

Fig. 3 Heatmap *for BRAFV600E*, *CD133*, and *CDX2* immunohistochemical staining results among 115 CRC tissues. Background (indicated by shade 0) represents negative staining for *BRAFV600E*, no loss of *CDX2* expression, and low *CD133* expression

studies have been conducted on mCRC patients revealing 7% prevalence in the Japanese population and 5.8% *BRAFV600E* positivity in a research done on the Chinese cohort [28, 29]. In comparison with reported studies, the present study revealed a high frequency of aberrations in *the BRAF* gene with 12% *BRAFV600E* mutations, reflecting the dire need for further studies on these mutations in the Pakistani population. Additional interesting findings included SNPs which have been reported on the ClinVar database as pathogenic or likely pathogenic in conditions other than CRC. Furthermore, previously unreported large deletions have been identified, which may have implications for potential personalized therapies. While studies have investigated oncogenic deletions within the kinase domain of *BRAF*, deletions specifically in exon 15 have not been documented [30]. As five amino

Table 3 Docking of wild-type and mutant BRAF proteins with the drugs encorafenib and vemurafenib

	Dock Score (Kcal/mol)			
Drugs	**Wild type**	**ZU-COL-27**	**ZU-COL-35**	**ZU-COL-37**
Encorafenib				
Tautomer 1	-3.199	-3.146	-0.706	-2.462
Tautomer 2	2.970	2.029	-0.311	-1.630
Vemurafenib				
Tautomer 1	-5.426	-2.569	-0.058	-3.564
Tautomer 2	-	-	-	-
Tautomer 3	-	-	-	-

*LigPre application in maestro software was used to prepare tautomers for the drugs (encorafenib and vemurafenib)

acids coded by exon 15 are involved in binding with the ligand, a large deletion in exon 15 affects the coding region of these amino acids. We observed through an induced fit docking study that the drugs were unable to bind with the protein due to the deletion in the exon 15 coding region. This finding warrants further investigation into a spectrum of mutations in the *BRAF* gene and their effect on therapy for optimal personalized management of such cases.

Piton et al. conducted a study to explore the use of IHC as a potential alternative to molecular techniques. They found that *BRAF* IHC has a sensitivity and specificity of 100% in detecting *V600E* mutations [19]. Galuppini et al. in a similar investigation reported that *BRAF* IHC had a sensitivity of 97% and specificity of 97.6% [31]. In the present study, it was observed that IHC detected all *BRAFV600E* mutations that were identified on sequencing. This finding is vital for economically disadvantaged countries like Pakistan where implementation of molecular techniques is not feasible.

High *CD133* expression observed in the present study aligns with existing literature that reports over-expression of *CD133* in CRC patients [32, 33]. The present study did not reveal an association of *CD133* with age or gender which is consistent with a study done by Kazama et al. [34]. However, a significant association of high *CD133* expression was observed with high grade, right-sidedness, advanced pathologic tumour stage, and presence of

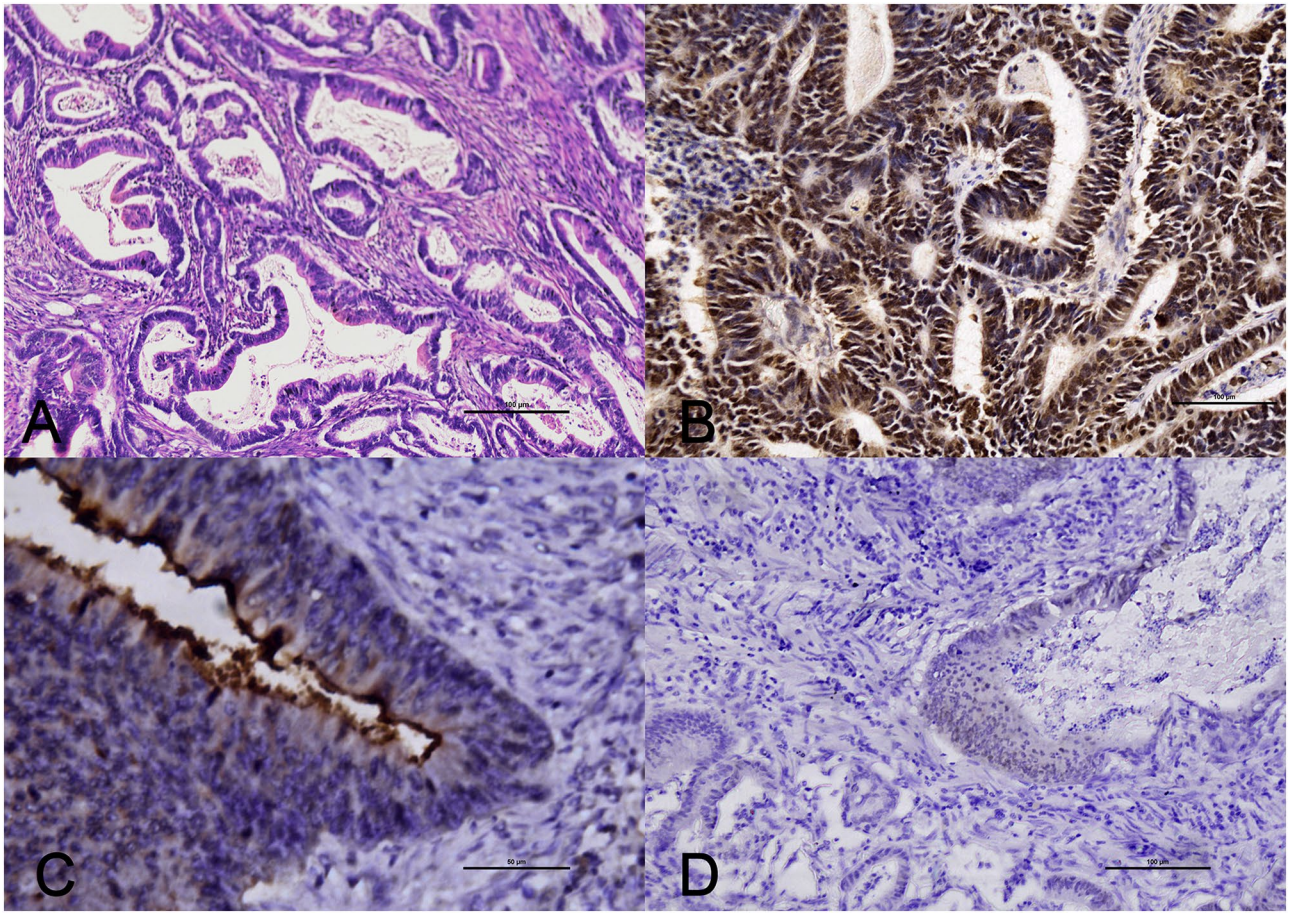

Fig. 4 The figure shows images of H& E and immunohistochemistry of colorectal carcinoma. **A**: H & E image of Colorectal Adenocarcinoma (*200x magnification).* **B**: Positive cytoplasmic staining of anti-*BRAFV600E* antibody (*200x magnification).* **C**: Positive *anti-CD133* antibody membranous staining on the luminal surface of glands (*400 x magnification).* **D**: Negative *CDX2* staining (*200x magnification)*

Table 4 Relationship of CD133 and CDX2 expression with demographic features

Clinicopathological Variables		*CD133* Expression				*CDX2* Expression			
		Low n (%)	High n (%)	OR (95% CI)	p-value	No Loss of *CDX2*	Loss of *CDX2*	OR (95% CI)	p-value
Age	< 50 years	49 (81.7%)	11 (18.3%)	1.243 (0.498–3.104)	0.65	48 (80%)	12 (20%)	0.889 (0.35–2.259)	0.818
	≥ 50 years	43(78.2%)	12(21.8%)			45 (81.8%)	10 (18.2%)		
Gender	Female	40(75.5%)	13 (24.5%)	0.592 (0.235–1.487)	0.350	41(77.4%)	12(22.6%)	0.657 (0.258–1.672)	0.477
	Male	52(83.9%)	10 (16.1%)			52(83.9%)	10(16.1%)		
Tumour Laterality	Right-sided	42(68.9%)	19 (31.1%)	0.177 (0.056–0.561)	**0.002**	46(75.4%)	15(24.6%)	0.457 (0.171–1.223)	0.155
	Left-sided	50 (92.6%)	4 (7.4%)			47(87%)	7(13%)		
Grade	Low	86(85.1%)	15(14.9%)	7.64 (2.321–25.182)	**0.001**	88(87.1%)	13(12.9%)	12.185 (3.531–42.049)	**< 0.001**
	High	6 (42.9%)	8 (57.1%)			5(35.7%)	9(64.3%)		
pT stage	T1-T3	85(85%)	15(15%)	6.476 (2.044–20.522)	**0.002**	85(85%)	15(15%)	4.985 (1.565–15.712)	**0.009**
	T4	7(46.7%)	8 (53.3%)			8(53.3%)	7(46.7%)		
PNI	No	85(83.3%)	17 (16.7%)	4.286 (1.28-14.349)	**0.022**	86(84.3%)	16(15.7%)	4.607 (1.368–15.512)	**0.017**
	Yes	7 (53.8%)	6 (46.2%)			7(53.8%)	6(46.2%)		
LVI	No	53(89.8%)	6 (10.2%)	3.85 (1.391–10.661)	**0.01**	51(86.4%)	8(13.6%)	2.125 (0.814–5.549)	0.156
	Yes	39(69.6%)	17 (30.4%)			42(75%)	14(25%)		

Chi Square/Fisher exact test applied. Significant results are given in bold $p \leq 0.05$. Test variables: age groups, gender, tumour laterality, grade, stage, PNI, LVI; Grouping variable: CD133 & CDX2 expression

Table 5 Association of BRAFV600E expression with CDX2 and CD133 expression

	BRAFV600E		Total	X^2	OR (95% CI)	*p*-value
	Negative	Positive				
CDX2						
No Loss	87(93.5%)	6(6.5%)	93(100%)	14.88	8.286 (2.497–27.498)	**0.001**
Loss	14(63.6%)	8(36.4%)	22(100)			
Total	101(87.8%)	14(12.2%)	115 (100%)			
CD133						
Low	88(95.7%)	4(4.3%)	92(100%))	26.351	16.923 (4.623–61.944)	**<0.001**
High	13(56.5%)	10 (43.5%)	23 (100%)			
Total	101(87.8%)	14(12.2%)	115 (100%)			

$p \leq 0.05$ Significant results denoted by bold text

lymphovascular, and perineural invasion. While Rey et al. have documented *CD133* overexpression to be associated with the location only, Ehtaram et al. have reported an association of *CD133* with gender, stage, and lymphovascular invasion [15, 35]. With growing emphasis on tailored therapy, studies have been done to identify drug targets based on *CD133* expression [13, 36]. Stemness has been speculated to follow differentiation defects. *CDX2*, a differentiation marker, has been reported to show partial or complete loss of expression in more than 20% of the CRC cases. A similar observation was made in the present study with loss of *CDX2* expression in 22 CRC cases (19.1%). Literature has documented *CDX2* loss to be associated with females and with the right-sided location of CRCs [8, 37]. However, we did not find any association of *CDX2* expression with gender or location. Consistent with the reported literature, a significant association was observed between *CDX2* expression and pathologic stage, grade and perineural invasion, which may be indicative of aggression and tumour progression [37, 38]. Differentiation defects in CRC have been associated with aggressiveness and recurrence of tumours which may be due to the proliferation of CSCs [39]. Tao et al. have reported that mutations resulting in differentiation defects and stemness promote *BRAFV600E*-driven carcinogenesis [40]. Furthermore, it has been documented that oncogenic *BRAFV600E* mutation and loss of differentiation disrupt the stemness-differentiation balance, restoring stem cell proliferation which creates a favourable environment for *BRAF*-driven oncogenesis [11, 40].

On performing univariate regression analysis, significant parameters were identified and further assessed in the final analysis using a multivariate logistic regression model. The univariate analysis showed a significant association of *BRAFV600E* with age, gender, tumour laterality, LVI, PNI and pathologic tumour stage while multivariate analysis revealed a significant association of advancing age and female gender with *BRAFV600E* mutations which has been documented in the published literature [28, 41, 42]. These findings suggest that female elderly patients should be particularly screened for possible *BRAFV600E* mutations. The significant association

Table 6 Binary logistic regression analysis for *BRAFV600E* mutation in colorectal adenocarcinoma cases ($n = 115$)

	Univariate Analysis		Multivariate Analysis	
Variable	**Crude OR (95% CI)**	**p-value**	**Adjusted OR (95% CI)**	**p-value**
Age	1.077 (1.028–1.129)	0.002	1.123 (1.024–1.232)	**0.014**
Gender				
Female	Reference		Reference	
Male	0.114 (0.024–0.536)	0.006	0.71 (0.006–0.831)	**0.035**
Tumour Laterality				
Right-sided	Reference		Reference	
Left-sided	0.157 (0.033–0.738)	0.019	1.201 (0.115–12.57)	0.879
Grade				
Low	Reference			
High	0.521 (0.063–4.319)	0.545	0.007 (0 -0.644)	**0.031**
pT stage				
T1-T3	Reference			
T4	7.667 (2.173–27.043)	0.002	0.159 (0.005–4.805)	0.29
LVI				
No	Reference		Reference	
Yes	4.563 (1.20-17.349)	0.026	10.025 (0.761-131.983)	0.08
PNI				
No	Reference		Reference	
Yes	4.089 (1.06-15.718)	0.04	2.648 (0.125–55.971)	0.532
CD 133				
Low expression	Reference		Reference	
High expression	16.923 (4.623–61.944)	< 0.001	65.649 (2.153-2001.55)	**0.016**
CDX2				
No loss	Reference		Reference	
Loss	8.286 (2.497–27.498)	0.001	8.621 (0.673-110.385)	0.098

considering the clinical value of grade, it has been included in the multivariate model; Multivariate analysis: $p \leq 0.05$; Significant p-value indicated by bold

of *BRAFV600E* with low-grade tumours may be because of a higher number of low-grade cases in our sample. The lack of association with high grade and stage of CRC indicates that genetic testing should not be reserved for advanced-stage cases only. Incorporation of IHC into routine histopathological practice may serve as a valuable tool for detecting genetic alterations. A significant association of *BRAFV600E* with high *CD133* expression and loss of *CDX2* was observed in univariate analysis. However multivariate regression analysis showed significant association with *CD133* and insignificant results with *CDX2*. The significant association of *BRAFV600E* with *CD133* raises the possibility of potential therapeutic intervention by anti-*CD133* drugs in *BRAF-driven* tumours that may otherwise be unlikely to respond to conventional therapy. Colorectal stemness has been associated with treatment resistance, recurrence, and aggressiveness of CRC [43]. The cases where conventional therapy does not offer a cure, the identification of CSCs using markers like *CD133* may be useful in defining therapeutic targets for CRC. Studies have reported *CD133* to be a useful predictive, prognostic, and therapeutic marker of CRC while *BRAFV600E* mutation itself may represent an actionable gene target, vital for personalized therapy in *BRAF*-mutant CRC patients [44, 45].

Due to the lack of population-specific data on molecular aberrations in CRC, stepping towards precision and target therapy in Pakistan remains a challenge. To our knowledge, this is the first study on *BRAF* mutations in the Pakistani population and opens avenues for identifying molecular targets based on our genetically distinct population. The concomitant high expression of *BRAFV600E* and *CD133* represents a vital molecular event to address in CRC. Identifying these molecular markers in CRC patients may help in the stratification of aggressive cases early in the course of the disease and target them for better treatment strategies. Furthermore, this study highlights the need for implementing molecular and genetic profiling early in the course of disease to identify our population-specific genetic aberrations. In economically challenged countries, IHC may provide a cost-effective and accessible solution to enhance diagnostic capabilities in lieu of molecular techniques for the detection of BRFA*V600E* mutations. The contribution of our study to existing information opens avenues for further research towards improvement in CRC therapeutics. The limitations of our study are the small sample size of *BRAFV600E*-positive patients and the absence of follow-up data. Moreover, due to a lack of distinction between localized and metastatic cases, the prognostic significance of *BRAFV600E* and *CD133* could not be ascertained. The effect of intronic variants and previously unreported mutations has not been thoroughly investigated. Since our primary focus was *BRAFV600E* mutations, we studied the partial sequence of exon 15 only. Further investigation using whole gene sequencing of *BRAF* might reveal a broader spectrum of clinically significant *BRAF* mutations. Studies based on tumours with background *BRAF* mutation, the associated molecular events, and treatment outcomes are warranted.

In conclusion, the frequency of *BRAF* mutations in our sample is alarmingly high. *BRAFV600E* mutation represents important molecular event that has been investigated in the Pakistani population and published in established databases through this study. Analysis of the samples encompassing novel large deletions showed alterations in the 3D structure of the protein, which ultimately affected the binding affinity of vemurafenib and encorafenib, reflecting the likely failure of BRAF

monotherapy in these cases. The spectrum of *BRAF* mutations identified in this study reflects the need for further investigations to initiate the targeted approach based on individual needs. Moreover, the strong association between *BRAFV600E* and *CD133* presents possible actionable genes that may offer better management of CRC patients through targeting stem cell proliferation along with anti-*BRAF* therapy.

Acknowledgements
The guidance and support of Ms. Fariha Anum, Ziauddin University, in sorting out statistics is acknowledged and appreciated.

Author contributions
All authors contributed to the study's conception and design. Material preparation and data collection were done by S.H., F.S and U.B.; analysis of gene sequencing was performed by S. H., and Am.K., analysis of IHC by S.H., T.M., and U.B. In silico studies of the Protein was conducted by As. K and Am.K. The first draft of the manuscript was written by S.H. Editing of the manuscript was done by S.H., T.M., Am. K, U.B., F.S. and As.K. All authors contributed to and approved the final manuscript.

Funding
The authors declare that no funds, grants, or other support were received during the preparation of this manuscript.

Data availability
The data sets generated during this study are available in Genbank NCBI with accession numbers: GenBank: PP003258.1; Pop Set: 2678087296[https://www.ncbi.nlm.nih.gov/nuccore/PP003258.1/;https://www.ncbi.nlm.nih.gov/popset/?term=2678087296].

Declarations

Ethical approval
The study was conducted in accordance with the Helsinki Declaration and was authorized by the Ethics Review Board, Ziauddin University, Karachi, Pakistan (2861120SHPAT29.01.2021).

Informed consent
Written informed consent was taken from study participants and the data collected was kept confidential.

Consent for publication
The anonymity of study participants is not compromised in any way as the personal information of the participants has been kept confidential and case numbers were assigned to each case to ensure that their identification is not revealed. Before performing the study, written informed consent was obtained from each participant. The consent form contained the information that data will be published without revealing names, addresses or telephone numbers of the participants.

Competing interests
The authors declare no competing interests.

Author details
[1]Department of Pathology, Ziauddin Medical University, Karachi 75000, Pakistan
[2]Research Department, Ziauddin Medical University Karachi, Karachi 75000, Pakistan
[3]Department of Molecular Medicine, Ziauddin Medical University Karachi, 4/B Shahrah-e-Ghalib Road, Block 6 Clifton, Karachi 75000, Pakistan
[4]Department of Pathology, Dow University of Health Sciences Karachi, Karachi 74200, Pakistan
[5]Dr. Panjwani Center for Molecular Medicine and Drug Research, International Center for Chemical and Biological Sciences, Jamil-ur-Rahman Center for Genome Research, University of Karachi, Karachi 75270, Pakistan

Received: 17 March 2024 / Accepted: 10 September 2024
Published online: 19 September 2024

References

1. Hossain MS, Karuniawati H, Jairoun AA, Urbi Z, Ooi DJ, John A, et al. Colorectal cancer: a review of carcinogenesis, global epidemiology, current challenges, risk factors, preventive and treatment strategies. Cancers. 2022;14(7):1732. https://doi.org/10.3390/cancers14071732.
2. Van der Jeught K, Xu H-C, Li Y-J, Lu X-B, Ji G. Drug resistance and new therapies in colorectal cancer. World J Gastroenterol. 2018;24(34):3834. https://doi.org/10.3748/wjg.v24.i34.3834.
3. Guan WL, Qiu MZ, He CY, Yang LQ, Jin Y, Wang ZQ, et al. Clinicopathologic features and prognosis of *BRAF* mutated Colorectal Cancer patients. Front Oncol. 2020;10:563407. https://doi.org/10.3389/fonc.2020.563407.
4. Chang X-n, Shang F-m, Jiang H-y, Chen C, Zhao Z-y, Deng S-h, et al. Clinicopathological features and prognostic value of kras/nras/*BRAF* mutations in colorectal cancer patients of central China. Curr Med Sci. 2021;41:118–26. https://doi.org/10.1007/s11596-021-2326-1.
5. Dao V, Heestand G. Beyond EGFR inhibitors in advanced colorectal cancer: Targeting *BRAF* and HER2. Curr Probl Cancer. 2023;100960. https://doi.org/10.1016/j.currproblcancer.2023.100960.
6. Malki A, ElRuz RA, Gupta I, Allouch A, Vranic S, Al Moustafa AE. Molecular mechanisms of Colon cancer progression and metastasis: recent insights and advancements. Int J Mol Sci. 2020;22(1). https://doi.org/10.3390/ijms22010130.
7. Kopetz S, Grothey A, Yaeger R, Van Cutsem E, Desai J, Yoshino T, et al. Encorafenib, binimetinib, and cetuximab in *BRAF V600E*–mutated colorectal cancer. N Engl J Med. 2019;381(17):1632–43. https://doi.org/10.1056/nejmoa1908075.
8. Tomasello G, Barni S, Turati L, Ghidini M, Pezzica E, Passalacqua R, et al. Association of *CDX2* expression with survival in early colorectal cancer: a systematic review and meta-analysis. J Clin Colorectal cancer. 2018;17(2):97–103.
9. Graule J, Uth K, Fischer E, Centeno I, Galván JA, Eichmann M, et al. *CDX2* in colorectal cancer is an independent prognostic factor and regulated by promoter methylation and histone deacetylation in tumours of the serrated pathway. Clin Epigenetics. 2018;10(1):120. https://doi.org/10.1186/s13148-018-0548-2.
10. Choi HB, Pyo J-S, Son S, Kim K, Kang G. Diagnostic and prognostic roles of *CDX2* immunohistochemical expression in colorectal cancers. Diagnostics. 2022;12(3):757.
11. Tong K, Pellón-Cárdenas O, Sirihorachai VR, Warder BN, Kothari OA, Perekatt AO, et al. Degree of tissue differentiation dictates susceptibility to *BRAF*-driven colorectal cancer. Cell Rep. 2017;21(13):3833–45. https://doi.org/10.1016/j.celrep.2017.11.104.
12. Das PK, Islam F, Lam AK. The roles of cancer stem cells and therapy resistance in colorectal carcinoma. Cells. 2020;9(6):1392. https://doi.org/10.3390/cells9061392.
13. Yuan Z, Liang X, Zhan Y, Wang Z, Xu J, Qiu Y, et al. Targeting *CD133* reverses drug-resistance via the AKT/NF-κB/MDR1 pathway in colorectal cancer. J Br J cancer. 2020;122(9):1342–53.
14. Liou G-Y, biology c. *CD133* as a regulator of cancer metastasis through the cancer stem cells. J Int J Biochem. 2019;106:1–7. https://doi.org/10.1038/s41416-020-0783-0.
15. Rey I, Putra A, Lindarto D, Yusuf F. Association between *CD133* expression and clinicopathological profile in colorectal cancer. J Med Glas. 2020;17(2):304–9. https://doi.org/10.17392/1106-20.
16. Asadzadeh Z, Mansoori B, Mohammadi A, Kazemi T, Mokhtarzadeh A, Shanehbandi D, et al. The combination effect of Prominin1 (*CD133*) suppression and oxaliplatin treatment in colorectal cancer therapy. Biomed Pharmacother. 2021;137:111364. https://doi.org/10.1016/j.biopha.2021.111364.
17. Bozorg-Ghalati F, Hedayati M, Dianatpour M, Mosaffa N, Azizi F. Targeting the *BRAF* signaling pathway in *CD133*pos cancer stem cells of anaplastic thyroid carcinoma. Asian Pac J Cancer Prevention: APJCP. 2019;20(5):1353. https://doi.org/10.31557/APJCP.2019.20.5.1353.
18. Bando H, Ohtsu A, Yoshino T. Therapeutic landscape and future direction of metastatic colorectal cancer. Nat Rev Gastroenterol Hepatol. 2023;20(5):306–22. https://doi.org/10.1038/s41575-022-00736-1.
19. Piton N, Borrini F, Bolognese A, Lamy A, Sabourin JC. KRAS and *BRAF* Mutation detection: is immunohistochemistry a possible alternative to Molecular

Biology in Colorectal Cancer? Gastroenterol Res Pract. 2015;2015:753903. https://doi.org/10.1155/2015/753903.
20. Ribeirinho-Soares S, Pádua D, Amaral AL, Valentini E, Azevedo D, Marques C, et al. Prognostic significance of MUC2, *CDX2* and SOX2 in stage II colorectal cancer patients. BMC Cancer. 2021;21(1):1–13.
21. Sun Y, Lai X, Yu Y, Li J, Cao L, Lin W et al. Inhibitor of DNA binding 1 (Id1) mediates stemness of colorectal cancer cells through the Id1-c-Myc-PLAC8 axis via the Wnt/β-catenin and shh signaling pathways. Cancer management research (Wash D C). 2019:6855–69. https://doi.org/10.2147/cmar.s207167
22. Gelsomino F, Casadei-Gardini A, Rossini D, Boccaccino A, Masi G, Cremolini C, et al. The role of anti-angiogenics in pre-treated metastatic *BRAF*-mutant colorectal cancer: a pooled analysis. Cancers (Basel). 2020;12(4):1022. https://doi.org/10.3390/cancers12041022.
23. Garcia-Carbonero N, Martinez-Useros J, Li W, Orta A, Perez N, Carames C, et al. KRAS and *BRAF* mutations as prognostic and predictive biomarkers for standard chemotherapy response in metastatic colorectal cancer: a single institutional study. Cells. 2020;9(1):219. https://doi.org/10.3390/cells9010219.
24. Bagadi SB, Sanghvi M, Nair SB, Das BR. Combined mutational analysis of KRAS, NRAS and *BRAF* genes in Indian patients with colorectal carcinoma. Int J Biol Markers. 2012;27(1):27–33. https://doi.org/10.5301/JBM.2012.9108.
25. Bagci B, Sari M, Karadayi K, Turan M, Ozdemir O, Bagci G. KRAS, BRAF oncogene mutations and tissue specific promoter hypermethylation of tumour suppressor SFRP2, DAPK1, MGMT, HIC1 and p16 genes in colorectal cancer patients. Cancer Biomark. 2016;17(2):133–43. https://doi.org/10.3233/cbm-160624.
26. Poulsen TS, de Oliveira D, Espersen MLM, Klarskov LL, Skovrider-Ruminski W, Hogdall E. Frequency and coexistence of KRAS, NRAS, *BRAF* and PIK3CA mutations and occurrence of MMR deficiency in Danish colorectal cancer patients. Apmis. 2021;129(2):61–9. https://doi.org/10.1111/apm.13091.
27. Alharbi A, Bin Dokhi H, Almuhaini G, Alomran F, Masuadi E, Alomran N. Prevalence of colorectal cancer biomarkers and their impact on clinical outcomes in Riyadh, Saudi Arabia. PLoS ONE. 2021;16(5):e0249590. https://doi.org/10.1371/journal.pone.0249590.
28. Ikoma T, Shimokawa M, Kotaka M, Matsumoto T, Nagai H, Boku S, et al. Clinical and prognostic features of patients with detailed RAS/*BRAF*-mutant colorectal cancer in Japan. BMC Cancer. 2021;21(1):518. https://doi.org/10.1186/s12885-021-08271-z.
29. Xu T, Li J, Wang Z, Zhang X, Zhou J, Lu Z, et al. Real-world treatment and outcomes of patients with metastatic BRAF mutant colorectal cancer. Cancer Med. 2023;12(9):10473–84. https://doi.org/10.1002/cam4.5783.
30. Foster SA, Whalen DM, Özen A, Wongchenko MJ, Yin J, Yen I, et al. Activation mechanism of oncogenic deletion mutations in *BRAF*. EGFR HER2 Cancer cell. 2016;29(4):477–93. https://doi.org/10.1016/j.ccell.2016.02.010.
31. Galuppini F, Pennelli G, Loupakis F, Lanza C, Vianello L, Sacchi D, et al. BRAF p.V600E-specific immunohistochemical assessment in colorectal cancer endoscopy biopsies is consistent with the mutational profiling. Histopathology. 2017;71(6):1008–11.
32. Chai X, Wu X, Ren J, Du K, Wu X, Feng F, et al. Expression of HIF-1α, ANXA3, *CD133* and their associations with clinicopathological parameters in human colon carcinoma. J Translational Cancer Res. 2022;11(6):1644. https://doi.org/10.21037/tcr-22-1277.
33. Park YY, An CH, Oh ST, Chang ED, Lee J. Expression of *CD133* is associated with poor prognosis in stage II colorectal carcinoma. J Med. 2019;98(32). https://doi.org/10.1097/md.0000000000016709.
34. Kazama S, Kishikawa J, Kiyomatsu T, Kawai K, Nozawa H, Ishihara S, et al. Expression of the stem cell marker *CD133* is related to tumour development in colorectal carcinogenesis. Asian J Surg. 2018;41(3):274–8. https://doi.org/10.1016/j.asjsur.2016.12.002.
35. Ehteram H, Aslanbeigi F, Ghoochani Khorasani E, Tolouee M, Haddad Kashani H. Expression and prognostic significance of stem cell marker *CD133* in survival rate of patients with colon cancer. Oncol Ther. 2022;10(2):451–61. https://doi.org/10.1007/s40487-022-00205-4.
36. Li W, Wang Z, Gao T, Sun S, Xu M, Pei R. Selection of *CD133*-targeted DNA aptamers for the efficient and specific therapy of colorectal cancer. J Mater Chem B. 2022;10(12):2057–66. https://doi.org/10.1039/d1tb02729h.
37. Asgari-Karchekani S, Karimian M, Mazoochi T, Taheri MA, Khamehchian T. CDX2 protein expression in Colorectal Cancer and ItsCorrelation with Clinical and pathological characteristics, prognosis, and Survival Rate of patients. J Gastrointest Cancer. 2020;51(3):844–9. https://doi.org/10.1007/s12029-019-00314-w.
38. Dawson H, Galván JA, Helbling M, Muller DE, Karamitopoulou E, Koelzer VH, et al. Possible role of *CDX2* in the serrated pathway of colorectal cancer characterized by *BRAF* mutation, high-level CpG island methylator phenotype and mismatch repair-deficiency. Int J Cancer. 2014;134(10):2342–51. https://doi.org/10.3389/fonc.2013.00265.
39. Tarazona N, Gimeno-Valiente F, Gambardella V, Huerta M, Rosello S, Zuniga S, et al. Detection of postoperative plasma circulating tumour DNA and lack of *CDX2* expression as markers of recurrence in patients with localised colon cancer. ESMO open. 2020;5(5):e000847. https://doi.org/10.1136/esmoopen-2020-000847.
40. Tao Y, Kang B, Petkovich DA, Bhandari YR, In J, Stein-O', Brien G et al. Aging-like spontaneous epigenetic silencing facilitates Wnt activation, stemness, and *BRAFV600E*-induced tumourigenesis. J Cancer cell. 2019;35(2):315 – 28. e6. https://doi.org/10.1016/j.ccell.2019.01.005.
41. Afrasanie VA, Marinca MV, Alexa-Stratulat T, Gafton B, Paduraru M, Adavidoaiei AM, et al. KRAS, NRAS, *BRAF*, HER2 and microsatellite instability in metastatic colorectal cancer - practical implications for the clinician. Radiol Oncol. 2019;53(3):265–74. https://doi.org/10.2478/raon-2019-0033.
42. Leach JD, Vlahov N, Tsantoulis P, Ridgway RA, Flanagan DJ, Gilroy K, et al. Oncogenic *BRAF*, unrestrained by TGFβ-receptor signalling, drives right-sided colonic tumourigenesis. Nat Commun. 2021;12(1):3464. https://doi.org/10.1038/s41467-021-23717-5.
43. Visioli A, Giani F, Trivieri N, Pracella R, Miccinilli E, Cariglia MG, et al. Stemness underpinning all steps of human colorectal cancer defines the core of effective therapeutic strategies. J EBioMedicine. 2019;44:346–60. https://doi.org/10.1016/j.ebiom.2019.04.049.
44. Huang R, Mo D, Wu J, Ai H, Lu Y. *CD133* expression correlates with clinicopathologic features and poor prognosis of colorectal cancer patients: an updated meta-analysis of 37 studies. J Med. 2018;97(23). https://doi.org/10.1097/md.0000000000010446.
45. Taieb J, Shi Q, Pederson L, Alberts S, Wolmark N, Van Cutsem E, et al. Prognosis of microsatellite instability and/or mismatch repair deficiency stage III colon cancer patients after disease recurrence following adjuvant treatment: results of an ACCENT pooled analysis of seven studies. Ann Oncol. 2019;30(9):1466–71. https://doi.org/10.1038/s41416-019-0526-2.

Publisher's note